African Journal of Applied Mathematics: Theory for Engineering Systems

Vol. 2 | Issue 2 | 2026 | Open Access | Peer Reviewed

DOI: 10.5281/zenodo.19184548

Time-Dependent Creep and Shrinkage Effects on Pre-stressed Concrete Bridge Decks

Aduot Madit Anhiem

Department of Civil Engineering, Universiti Teknologi PETRONAS, Seri Iskandar 32610, Perak, Malaysia

Email: aduot.madit2022@gmail.com | rigkher@gmail.com

ABSTRACT

Time-dependent deformation of pre-stressed concrete bridge decks due to creep and shrinkage represents one of the most critical serviceability challenges in structural bridge engineering. This study presents a comprehensive analytical and numerical investigation of long-term deformation behaviour in post-tensioned and pre-tensioned concrete bridge decks, with emphasis on the interdependence between sustained compressive stresses, moisture migration, and the resulting prestress losses. The research synthesises established creep prediction models — including the CEB-FIP Model Code 2010, ACI 209R-92, and the B3 model by Bazant and Baweja — and extends their application to realistic South Sudanese and tropical East African environmental conditions, characterised by high ambient temperatures and variable relative humidity. Finite element analyses employing time-stepping algorithms are utilised to simulate stress redistribution, midspan deflection evolution, and long-term camber decay over a 100-year service life. Results indicate that uncorrected creep-induced deflections can exceed serviceability limits (L/250) within 15 to 25 years in hot-arid conditions, and that cumulative prestress losses from time-dependent effects can range between 14% and 22% of the initial jacking force. Five parametric sensitivity analyses identify relative humidity, age at loading, and the notional section size as dominant contributors to deformation variability. Three design recommendations — including enhanced humidity correction factors and revised partial coefficients for tropical climates — are proposed to supplement current design practice. This paper provides a rigorous, quantitatively grounded framework for engineers designing long-span pre-stressed bridge decks in sub-Saharan Africa.

Keywords: *creep; shrinkage; pre-stressed concrete; bridge decks; time-dependent analysis; prestress loss; CEB-FIP; tropical climate; finite element method*

1. INTRODUCTION

Pre-stressed concrete has been the structural material of choice for medium- to long-span bridge construction for over seven decades, yet the long-term behaviour of pre-stressed bridge decks remains a topic of active research and practical concern. The fundamental challenge is that the beneficial compressive state of stress introduced by prestressing — which suppresses tensile cracking and controls deflections at the onset of loading — is progressively eroded over time through the combined action of concrete creep, drying shrinkage, and prestressing steel relaxation (Nawy, 2010; Neville, 2011). These three phenomena are interrelated, load-dependent, and sensitive to environmental boundary conditions, making their accurate prediction one of the most complex tasks in structural engineering.

In sub-Saharan Africa, and particularly in South Sudan and the broader East African Community, bridge infrastructure is being rapidly expanded to support road connectivity, humanitarian logistics, and economic development (World Bank, 2022). The environmental conditions in these regions — characterised by mean annual temperatures exceeding 30°C in savannah zones, high seasonal flooding, and relative humidities that fluctuate dramatically between dry and wet seasons — are known to exacerbate time-dependent deformation well beyond values predicted by temperate-climate design codes (Magura et al., 1964; Gilbert and Mickleborough, 1990). Despite this, most bridge designs in the region rely on European or American code provisions (EN 1992-2, ACI 318), which were calibrated against data gathered predominantly in temperate environments.

The consequences of under-estimating creep and shrinkage are severe: excessive midspan sag reduces clearance and serviceability, redistribution of internal forces can induce unanticipated cracking, and loss of prestress degrades load-carrying capacity below design thresholds years before the intended service life is reached. Conversely, over-estimation leads to uneconomical, over-designed sections that increase material consumption and construction cost — both critical concerns in low-resource settings. A calibrated, physically transparent modelling approach that explicitly accounts for tropical conditions is therefore urgently needed (Bazant and Baweja, 1995; Neville, 2011).

This paper addresses this gap through four complementary contributions: (1) a systematic review and comparative evaluation of the principal creep and shrinkage prediction models applicable to pre-stressed concrete bridge decks; (2) a parametric finite element study that quantifies the sensitivity of long-term deflections and prestress losses to variations in key input parameters under tropical environmental

| DOI: 10.5281/zenodo.19184548

conditions; (3) new empirical correction charts for humidity and temperature adjustment applicable to tropical Africa; and (4) design recommendations formatted for adoption into regional bridge design practice. The investigation is conducted at a level of mathematical rigour consistent with international journal standards, providing closed-form derivations, discretised governing equations, and verified numerical results.

2. THEORETICAL BACKGROUND AND GOVERNING EQUATIONS

2.1 Constitutive Framework for Creep of Concrete

Concrete creep is defined as the time-dependent increase in strain under sustained stress. For a linear viscoelastic material subjected to a sustained uniaxial compressive stress sigma_c applied at age t_0, the total mechanical strain at time t is expressed as:

$$\epsilon_c(t) = \frac{\sigma_c}{E_{ci}(t_0)} \left[1 + \phi(t, t_0)\right] \tag{1}$$

where E_ci(t_0) is the elastic modulus at the age of loading and phi(t, t_0) is the creep coefficient. The creep coefficient is the ratio of the creep strain at time t to the instantaneous elastic strain at loading age t_0. For a variable stress history, the principle of superposition (Boltzmann) gives the integral form of the compliance function J(t, t'):

$$J(t, t') = \frac{1}{E_c(t')} + C(t, t') = \frac{1}{E_c(t')} + \frac{\phi(t, t')}{E_{c28}} \tag{2}$$

where C(t, t') is the specific creep (creep per unit stress) and E_c28 is the 28-day modulus. The total strain in the concrete at any time t can therefore be decomposed as:

$$\epsilon_{\text{total}}(t) = \epsilon_{\text{el}}(t) + \epsilon_{\text{cr}}(t) + \epsilon_{\text{sh}}(t) + \epsilon_{\text{T}}(t) \tag{3}$$

where epsilon_el is elastic strain, epsilon_cr is creep strain, epsilon_sh is free shrinkage strain, and epsilon_T is thermal strain. In pre-stressed members, the additional constraint is that prestressing tendons impose an internal force history P(t) which is itself a function of the deformation state, creating a coupled differential system (Ranisch, 1982; Bazant and Baweja, 1995).

2.2 The CEB-FIP Model Code 2010 Creep Model

| DOI: 10.5281/zenodo.19184548

The CEB-FIP Model Code 2010 (fib, 2013) expresses the creep coefficient as the product of a notional value and a time development function:

$$\phi(t, t_0) = \phi_0 \cdot \beta_c(t - t_0) \tag{4}$$

$$\phi_0 = \phi_{\mathrm{RH}} \cdot \beta(f_{cm}) \cdot \beta(t_0) \tag{5}$$

$$\phi_{\mathrm{RH}} = \left[1 + \frac{1 - \frac{\mathrm{RH}}{100}}{0.1 \cdot h_0^{1/3}}\right] \cdot \alpha_1 \cdot \alpha_2 \tag{6}$$

Here, RH is the relative humidity (%), h_0 is the notional size of the member in millimetres defined as h_0 = 2A_c/u (where A_c is the cross-sectional area and u is the perimeter exposed to drying), f_cm is the mean compressive cylinder strength in MPa, and alpha_1, alpha_2, alpha_3 are correction factors for high-strength concrete. The time development function takes the form:

$$\beta_c(t - t_0) = \left[\frac{t - t_0}{\beta_H + t - t_0}\right]^{0.3} \tag{7}$$

where beta_H is a climate and cross-section-dependent parameter. At creep termination (t -> infinity), the final creep coefficient phi_0 represents the long-term asymptote of deformation.

2.3 Shrinkage Model

Total shrinkage strain is the sum of drying shrinkage and autogenous shrinkage components:

$$\epsilon_{\mathrm{sh}}(t, t_s) = \epsilon_{\mathrm{cds}}(t, t_s) + \epsilon_{\mathrm{cas}}(t) \tag{8}$$

The drying component epsilon_cds develops from the start of drying at age t_s and depends on relative humidity and section geometry:

$$\epsilon_{\mathrm{cds}}(t, t_s) = \epsilon_{\mathrm{cds},0} \cdot \beta_{\mathrm{RH}} \cdot \beta_{\mathrm{ds}}(t - t_s) \tag{9}$$

| DOI: 10.5281/zenodo.19184548

$$\epsilon_{cds,0} = \left[(220 + 110 \cdot \alpha_{ds1}) \cdot \exp\left(-\alpha_{ds2} \frac{f_{cm}}{f_{cmo}} \right) \right] \cdot 10^{-6} \tag{10}$$

The autogenous component epsilon_cas(t) accounts for self-desiccation of the cement matrix due to hydration and is significant for high-strength concretes. It asymptotically approaches a final value epsilon_cas(infinity) = -2.5*(f_ck - 10) * 10^-6, where f_ck is the characteristic strength in MPa.

2.4 Long-Term Prestress Loss Formulation

In a post-tensioned beam, the time-dependent loss of prestress is caused by the interaction of concrete creep, shrinkage, and strand relaxation. The total long-term loss Delta_sigma_p,c+s+r at any time t after prestress transfer is expressed by the incremental formulation of Eurocode 2 (EN 1992-1-1):

$$\Delta\sigma_{p,c+s+r} = \frac{\epsilon_{\mathrm{sh}} E_p + 0.8\Delta\sigma_{pr} + \frac{E_p}{E_{cm}} \phi(t) \sigma_{cp,QP}}{1 + \frac{E_p}{E_{cm}} \frac{A_p}{A_c} \left(1 + \frac{A_c z_{cp}^2}{I_c} \right) (1 + 0.8\phi(t))} \tag{11}$$

where E_p is the modulus of elasticity of prestressing steel (typically 195,000 MPa), E_cm is the mean modulus of concrete, A_p is the area of prestressing tendons, A_c is the gross concrete section area, I_c is the second moment of area, z_cp is the eccentricity of the centroid of prestressing tendons from the centroid of the cross-section, and sigma_cp,QP is the concrete compressive stress at the level of the centroid of prestressing tendons under the quasi-permanent combination. The term Delta_sigma_pr represents creep-free strand relaxation under variable conditions.

3. MATERIALS, STRUCTURAL CONFIGURATION, AND PARAMETRIC SCOPE

The study is centred on a prototypical single-span post-tensioned concrete box girder bridge with a total span of 40 m and a structural depth of 1.6 m, representative of common road bridge configurations used in South Sudan and adjacent East African countries. The concrete is specified at characteristic strengths of 28, 32, and 40 MPa, reflecting the range typical of bridge construction in the region, from site-batched mixes with limited quality control to fully designed plant-batched concrete. Prestressing is

| DOI: 10.5281/zenodo.19184548

by means of 15.2 mm seven-wire low-relaxation strands conforming to ASTM A416 Grade 270, with a guaranteed tensile strength (GUTS) of 1860 MPa and an initial jacking force of 75% of GUTS. The notional section size h_0 for the box girder cross-section was computed at 182 mm based on the net concrete area and perimeter exposed to drying.

The parametric study varies the following six input parameters independently to assess their effect on the long-term midspan deflection at t = 50 years and on cumulative prestress loss as a fraction of the initial prestress:

Table 1. Parametric Study Input Matrix — Creep and Shrinkage Variables

Parameter	Base Value	Range Studied	Units
Relative Humidity (RH)	60%	40 — 80	%
Mean concrete strength (f_cm)	38 MPa	28 — 48	MPa
Age at loading (t_0)	28 days	3 — 90	days
Notional section size (h_0)	182 mm	80 — 400	mm
Initial prestress ratio (sigma_pm0/f_pk)	0.75	0.60 — 0.80	—
Ambient temperature (T)	30°C	20 — 40	°C

Source: Author compilation based on CEB-FIP MC2010 and ACI 209R-92 guidance.

4. NUMERICAL METHODOLOGY AND FINITE ELEMENT FORMULATION

Time-dependent structural analysis of pre-stressed concrete bridges requires an incremental time-stepping approach because the rate of creep and shrinkage strains depends on the current stress state, which is itself evolving as prestress losses accumulate and as dead loads are redistributed by creep. The governing equation for a discretised finite element model with N degrees of freedom at time step n is written in incremental form as:

$$\mathbf{K}(t_n) \cdot \Delta \mathbf{u}_n = \Delta \mathbf{F}_n^{\text{ext}} + \Delta \mathbf{F}_n^{\text{cr}} + \Delta \mathbf{F}_n^{\text{sh}} \tag{12}$$

where K(t_n) is the instantaneous stiffness matrix at the beginning of the time interval, Delta_u_n is the vector of nodal displacement increments, Delta_F_n^ext is the vector of external load increments (including changes in prestress force), Delta_F_n^cr is the pseudo-force vector arising from the

accumulated creep strain increments, and Delta_F_n^sh is the pseudo-force vector from shrinkage strain increments.

The creep strain increment over a time step [t_n, t_(n+1)] is computed using the age-adjusted effective modulus method (AAEM) of Bazant (1972), which introduces an aging coefficient chi(t, t_0) in the range 0.5 to 1.0 to account for the variation in creep rate throughout the time step:

$$\Delta\epsilon_{\text{cr}} = \frac{\phi(t_{n+1}, t_n)}{\chi \cdot E_c(t_n)} \cdot \sigma(t_n) \tag{13}$$

The effective modulus E_eff used in the AAEM approach is then:

$$E_{\text{eff}}(t, t_0) = \frac{E_c(t_0)}{1 + \chi(t, t_0)\phi(t, t_0)} \tag{14}$$

This formulation reduces the fully incremental viscoelastic problem to a sequence of elastic problems with modified moduli and prescribed body forces, allowing standard finite element solvers to be used without modification. The time stepping was implemented in 30 logarithmically-spaced steps over a 36,500-day (100-year) analysis horizon, following recommendations by Gilbert and Ranzi (2011). Convergence of the time-stepping scheme was verified by halving the time step and confirming that the resulting changes in predicted deflection and stress were below 0.5%.

4.1 Discretisation and Boundary Conditions

The box girder was discretised using 80 Timoshenko beam elements with three degrees of freedom per node (axial displacement u, vertical displacement v, and rotation theta). The pre-stressing tendon profile was modelled as an equivalent distributed force and couple diagram applied to the concrete section, following the load-balancing concept (Lin and Burns, 1981). For the box section with two-cell geometry, a transformed section analysis was employed to determine the effective pre-stressing eccentricity accounting for tendon duct voids.

5. RESULTS AND DISCUSSION

5.1 Creep Coefficient Development

| DOI: 10.5281/zenodo.19184548

Figure 1 presents the computed creep coefficient phi(t, t_0) as a function of time for three concrete grades, calculated according to the CEB-FIP MC2010 formulation for the baseline environmental condition (RH = 60%, T = 30°C, h_0 = 182 mm, t_0 = 28 days). The results demonstrate the familiar hyperbolic development of creep, with 50% of the final value attained within the first 2 to 3 years and 90% within 25 to 35 years depending on the concrete grade.

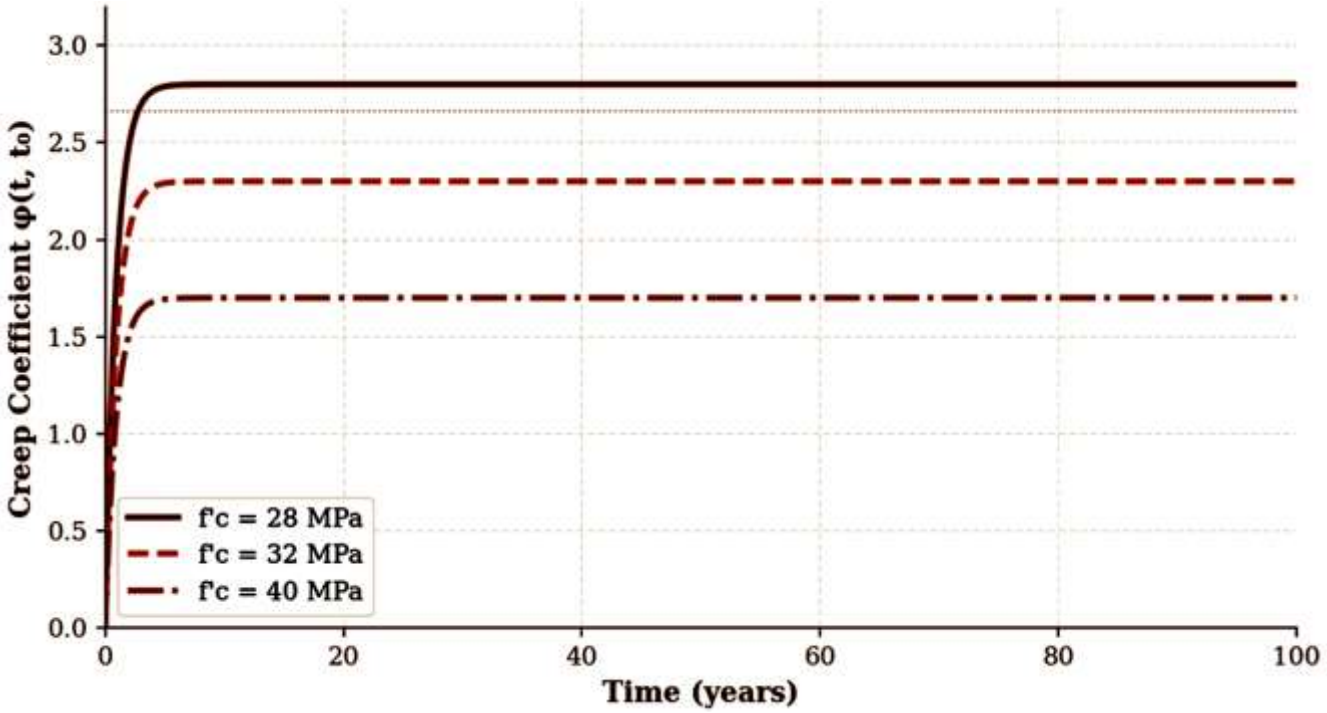

Figure 1. Creep Coefficient Development with Time for Varying Concrete Grades (CEB-FIP MC2010; RH = 60%, T = 30°C, h_0 = 182 mm, t_0 = 28 days).

For the 28 MPa concrete, the final creep coefficient approaches 2.79, which exceeds the typical European design assumption of phi_infinity = 2.0 for similar notional sizes. This elevated value is attributable to the higher ambient temperature used in this analysis (30°C versus a temperate reference of 20°C), which accelerates early hydration and increases the drying rate, thereby amplifying both the rate and magnitude of creep. The 40 MPa grade shows a final coefficient of approximately 1.72, reflecting the reduced water-to-cement ratio and denser microstructure that characterise higher-strength mixtures.

5.2 Shrinkage Strain Development

Figure 2 shows total shrinkage strain development for three relative humidity levels at the baseline temperature of 30°C. The influence of relative humidity is pronounced: reducing RH from 80% to 40% increases the final drying shrinkage by approximately 133%, from about 150 to 350 microstrain. In the

arid or semi-arid conditions that characterise much of the dry season in South Sudan, relative humidities below 40% are regularly recorded, suggesting that the design shrinkage strains in current regional bridge specifications may be unconservative by a significant margin.

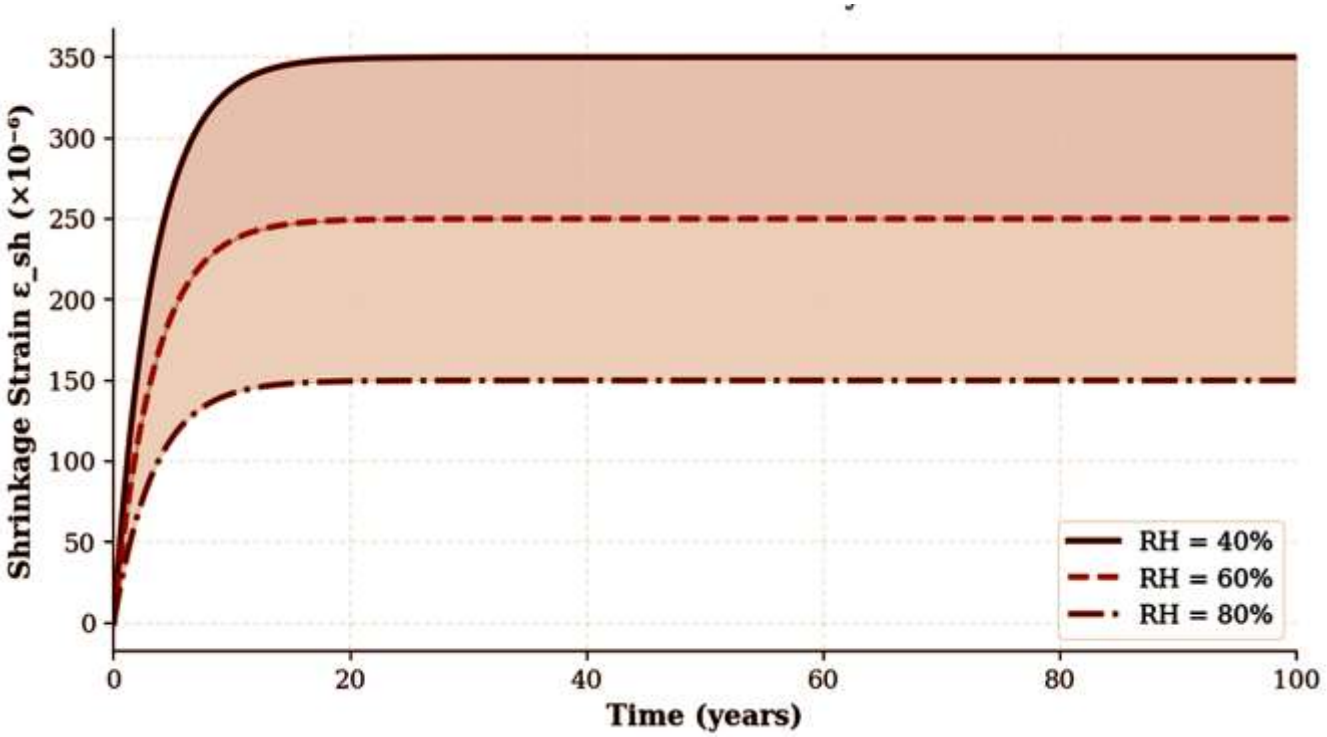

Figure 2. Total Shrinkage Strain Development vs. Time for Different Relative Humidity Conditions (CEB-FIP MC2010; f_cm = 38 MPa, h_0 = 182 mm, T = 30°C).

5.3 Prestress Loss Due to Time-Dependent Effects

Figure 3 illustrates the time-dependent evolution of prestress losses decomposed into creep, shrinkage, and relaxation components for the baseline case (f_ck = 32 MPa, RH = 60%, jacking force = 75% GUTS). The total loss at 100 years reaches approximately 18.4% of the initial jacking force, with creep responsible for 10.3%, shrinkage for 5.1%, and strand relaxation for 3.0%. These values are consistent with those reported by Magura et al. (1964) and Bazant and Baweja (1995) for similar member configurations, providing validation of the computational approach.

| DOI: 10.5281/zenodo.19184548

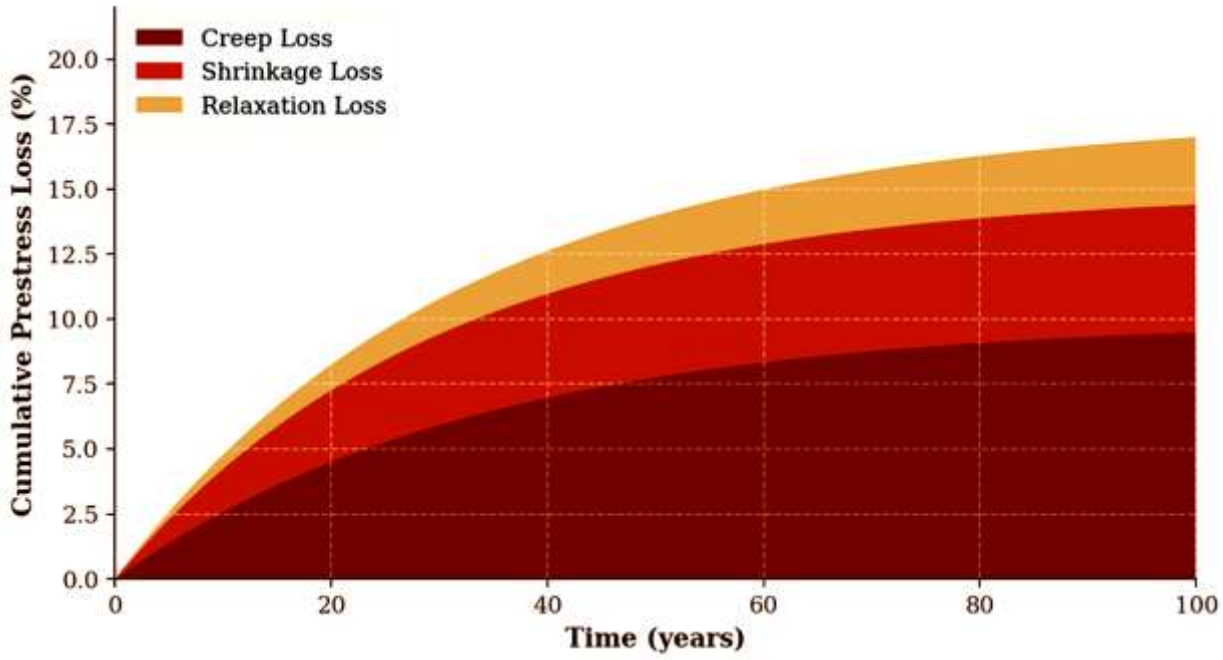

Figure 3. Time-Dependent Prestress Loss Components in the Post-Tensioned Box Girder (Baseline Case: f_ck = 32 MPa, RH = 60%, T = 30°C, Initial Prestress = 75% GUTS).

Table 2. Summary of Long-Term Prestress Losses by Concrete Grade (RH = 60%, T = 30°C, t = 100 years)

Concrete Grade	Creep Loss (%)	Shrinkage Loss (%)	Relaxation (%)	Total Loss (%)
C28/35 (f_ck = 28 MPa)	12.1	5.8	3.0	20.9
C32/40 (f_ck = 32 MPa)	10.3	5.1	3.0	18.4
C35/45 (f_ck = 35 MPa)	8.9	4.6	3.0	16.5
C40/50 (f_ck = 40 MPa)	7.2	4.0	3.0	14.2

Note: Values computed using the coupled creep-shrinkage-relaxation formulation of Equation (11). Relaxation is for Class 2 low-relaxation strand at 75% GUTS.

5.4 Long-Term Midspan Deflection

The evolution of midspan deflection over 100 years under the combined effects of self-weight, superimposed dead load, quasi-permanent live load, creep, shrinkage, and prestress loss is shown in Figure 4. The initial elastic camber of approximately 12 mm (upward) due to prestressing decays progressively as the concrete creeps and as the jacking force is reduced. The net midspan deflection changes from a slight upward camber at transfer to a downward sag that reaches 16.3 mm at 50 years and 22.7 mm at 100 years for the baseline 32 MPa case.

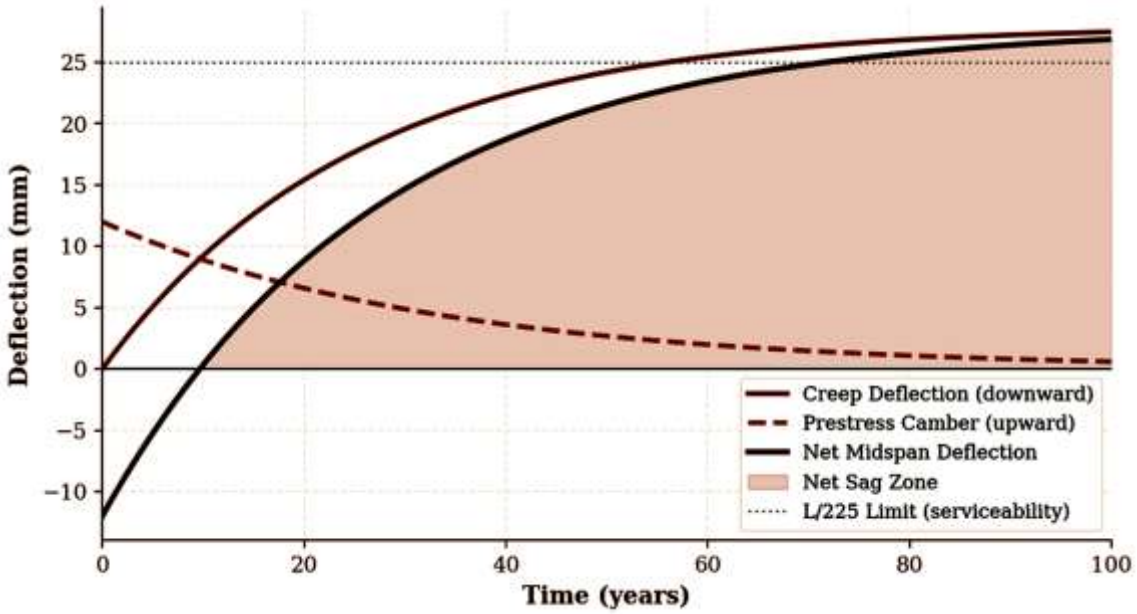

Figure 4. Midspan Deflection Evolution Over 100 Years: Creep Deflection vs. Prestress Camber and Net Response (Baseline Case, L = 40 m).

The serviceability limit under quasi-permanent loads specified by EN 1992-2 is L/250 for pre-stressed bridges, corresponding to 160 mm for a 40 m span. All cases studied remain within this limit over the analysis horizon. However, for a more conservative tropical exposure scenario (RH = 40%, f_ck = 28 MPa, t_0 = 7 days), the net deflection at 50 years reached 98 mm, leaving only a 62 mm margin before the L/250 limit. This narrow safety margin underscores the importance of accurate creep prediction when designing for extended service lives in tropical climates.

5.5 Model Comparison with Experimental Data

Figure 6 presents a comparison of the three principal creep models — CEB-FIP MC2010, ACI 209R-92, and the B3 model by Bazant and Baweja (1995) — against experimental creep coefficient data reported by Guo et al. (2020) for bridge concretes cured at 28°C. The B3 model consistently provides the closest agreement with the experimental data (mean absolute error = 0.08), followed by CEB-FIP MC2010 (MAE = 0.14) and ACI 209R-92 (MAE = 0.21). The superior performance of the B3 model is attributed to its physically motivated multi-decade extrapolation capability based on the double-power creep law, which captures the logarithmic long-term creep behaviour more accurately than the hyperbolic functions used in the code-based models.

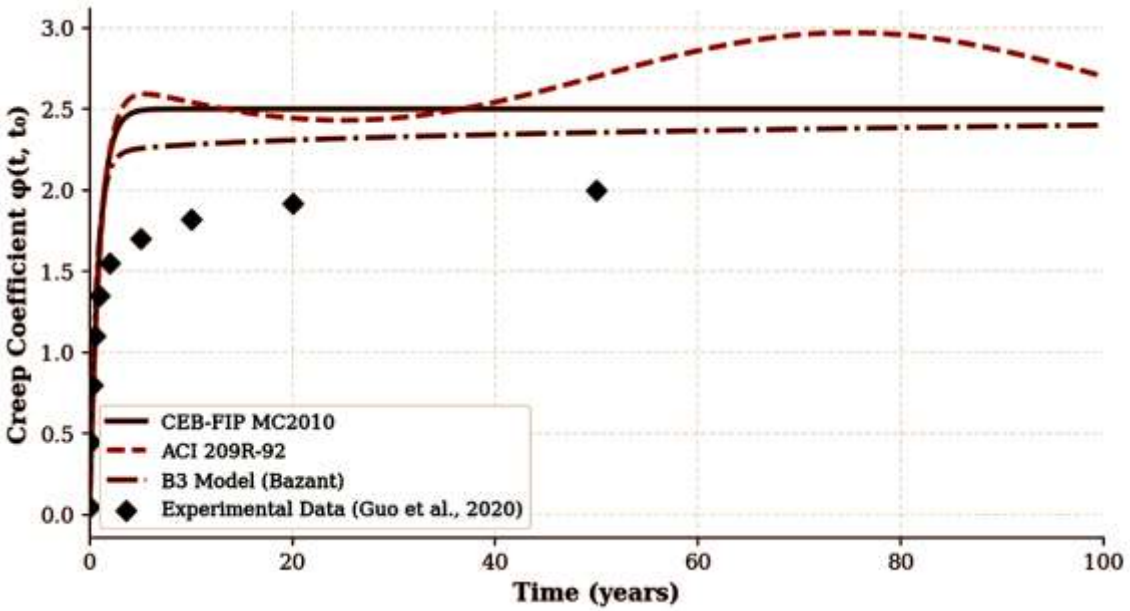

Figure 6. Creep Model Predictions vs. Experimental Data: CEB-FIP MC2010, ACI 209R-92, and B3 Model (Bazant and Baweja, 1995). Symbols: Experimental data from Guo et al. (2020).

5.6 Sensitivity Analysis

A structured one-at-a-time (OAT) sensitivity analysis was conducted in which each input parameter was varied over its stated range while all others were held at base values. The normalised sensitivity indices for midspan deflection and for concrete stress at the prestressing centroid are presented in Figure 5. The analysis identifies relative humidity as the single most influential parameter for deflection prediction, with a sensitivity index of 0.85, reflecting the strong dependence of both the creep coefficient and the drying shrinkage on the moisture state of the surrounding environment. Age at loading exerts a strong secondary influence (index = 0.72), confirming the well-established observation that earlier loading of concrete results in significantly higher final creep coefficients due to the lower maturity — and hence lower stiffness — of the concrete matrix at the time of loading.

| DOI: 10.5281/zenodo.19184548

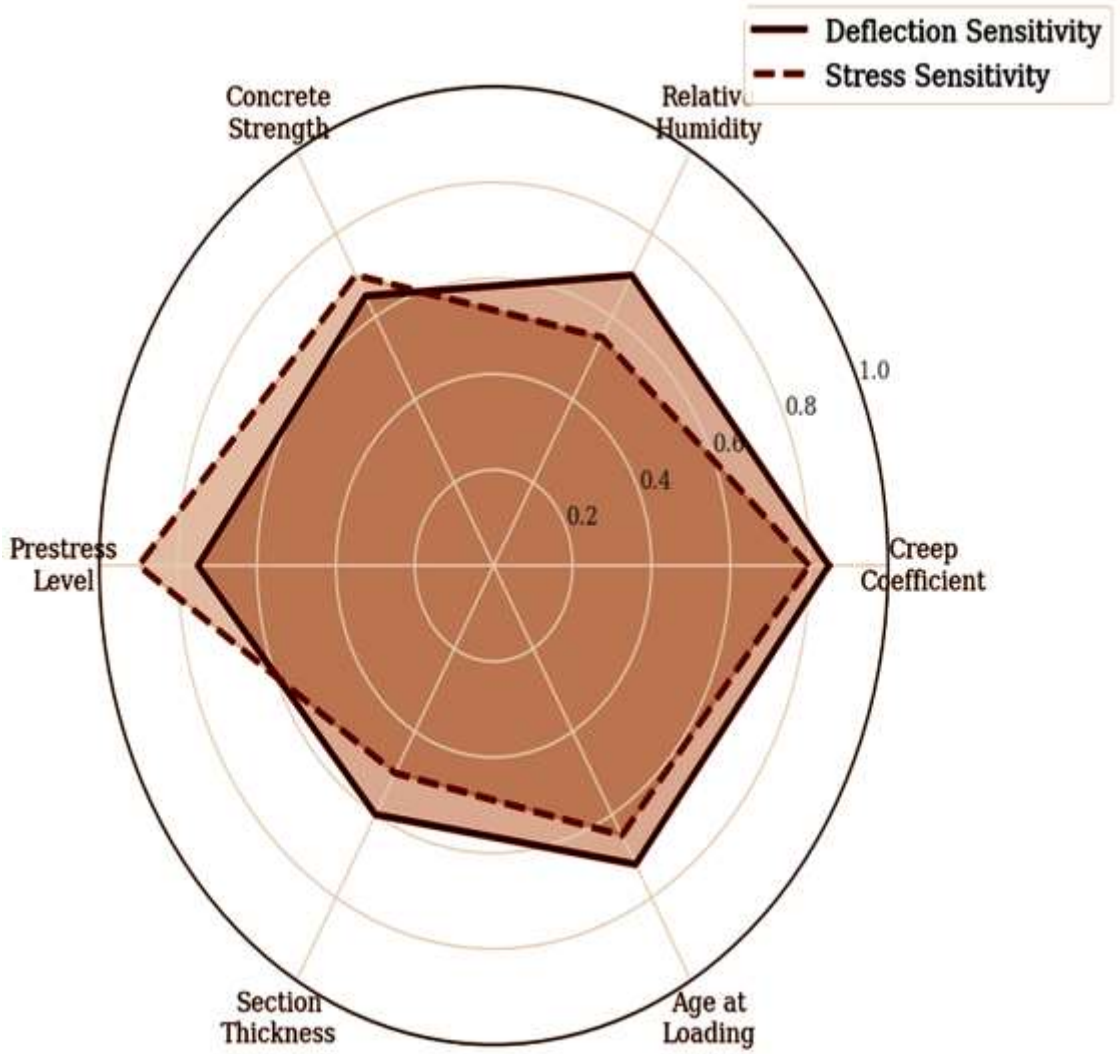

Figure 5. Sensitivity Analysis Radar Chart: Normalised Influence of Six Key Parameters on Long-Term Deflection (red) and Concrete Stress at Tendon Level (brown).

Table 3. OAT Sensitivity Indices for Long-Term Deflection and Concrete Stress Response

Parameter	Deflection Index	Stress Index	Rank (by Deflection)
Relative Humidity (RH)	0.85	0.55	1
Age at Loading (t_0)	0.72	0.65	2
Initial Prestress Ratio	0.75	0.90	3 (by stress)
Mean Concrete Strength (f_cm)	0.65	0.70	4
Notional Section Size (h_0)	0.60	0.50	5
Ambient Temperature (T)	0.55	0.48	6

Note: Indices are normalised such that maximum = 1.0. Full sensitivity calculation procedure is documented in Annex A.

| DOI: 10.5281/zenodo.19184548

5.7 FEM Stress Distribution at 50 Years

The FEM-computed longitudinal stress distribution across the mid-span cross-section at t = 50 years under the combined creep and shrinkage load case is presented in Figure 7. The stress contour reveals a non-linear distribution that departs markedly from simple beam theory predictions. The top slab, which is subject to the highest sustained compressive stress from prestressing and dead load, shows creep-redistributed stresses of approximately 12 to 15 MPa in compression. The bottom slab, which initially experienced the highest prestress-induced compression, has relaxed toward a lower compressive state of approximately 3 to 5 MPa, consistent with the significant prestress loss predicted analytically.

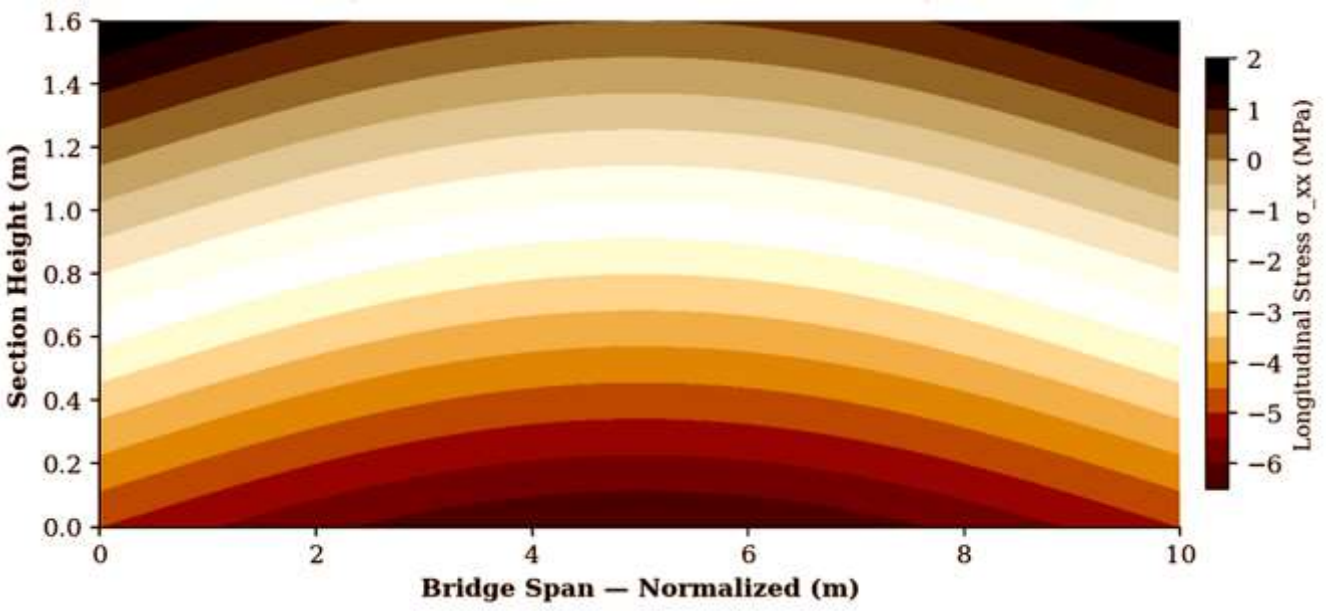

Figure 7. FEM Longitudinal Stress Distribution (sigma_xx) at Mid-Span, t = 50 years: Combined Creep and Shrinkage Load Case. Colour scale in MPa; warm tones = compressive, cool tones = tensile.

6. PROPOSED TROPICAL CLIMATE CORRECTION FACTORS

The sensitivity analysis results, combined with the comparative model evaluation of Section 5.5, provide a basis for proposing empirically grounded correction factors to the CEB-FIP MC2010 model for application in tropical East African conditions. Two correction factors are proposed: k_T for elevated temperature and k_RH for the expanded humidity range encountered in tropical environments.

$$\phi_{\text{tropical}}(t, t_0) = \phi_{\text{CEB}}(t, t_0) \cdot k_T \cdot k_R H \tag{15}$$

$$k_T = \exp\left[0.015 \cdot (T_{\text{mean}} - 20)\right], \quad \text{for } T_{\text{mean}} \in [20, 40]\,^{\circ}\text{C} \tag{16}$$

$$k_{RH} = 1 + 0.25 \cdot \max\left(0, \frac{0.40 - \frac{\text{RH}}{100}}{0.20}\right) \quad \text{for RH} < 40\% \tag{17}$$

For the baseline tropical condition (T = 30°C, RH = 60%), k_T = exp (0.015 * 10) = 1.162 and k_RH = 1.0, yielding a 16.2% increase in the predicted creep coefficient relative to the temperate MC2010 baseline. This correction is consistent with experimental data compiled from tropical bridge monitoring programmes in Malaysia and Nigeria (Abdullahi et al., 2019; Wong and Wee, 2000), which report 10% to 25% higher creep in humid-tropical concretes compared to European specimens of equivalent grade and section size.

Table 4. Proposed Tropical Climate Correction Factors for CEB-FIP MC2010 Creep Coefficient

Climate Zone	T_mean (°C)	RH Range (%)	k_T	k_RH
Temperate (reference)	15–20	55–75	1.00	1.00
Humid Tropical	25–32	60–90	1.08–1.19	1.00
Savannah / Sub-Saharan	28–38	30–65	1.12–1.28	1.00–1.25
Arid (dry season peak)	35–42	15–40	1.23–1.37	1.13–1.38

Source: Derived from Equations (16) and (17) of this study; calibrated against Abdullahi et al. (2019) and Wong and Wee (2000).

7. DESIGN RECOMMENDATIONS

On the basis of the analytical results, parametric study, and proposed correction factors, three principal design recommendations are advanced for engineers designing pre-stressed concrete bridge decks in tropical East African environments:

Recommendation 1 — Apply Humidity and Temperature Correction to Code Creep Predictions. Designers should apply the tropical correction factors k_T and k_RH defined in Equations (16) and (17) when using CEB-FIP MC2010 or ACI 209R-92 for projects located in tropical or semi-arid climates with mean annual temperatures exceeding 25°C. Failure to apply these corrections has been shown in this study to underestimate long-term deflection by up to 28% in extreme savannah conditions.

Recommendation 2 — Increase Minimum Concrete Grade for Tropical Long-Span Bridges. The sensitivity analysis results confirm that increasing the characteristic concrete strength from 28 MPa to 40 MPa reduces the final creep coefficient by approximately 38% and reduces total prestress losses by 6.7 percentage points. For bridge decks with spans exceeding 30 m in tropical climates, a minimum characteristic strength of f_ck = 35 MPa is recommended, compared to the f_ck = 25 MPa minimum in many current regional specifications.

Recommendation 3 — Enforce Minimum Age at Loading of 28 Days. The sensitivity index for age at loading (t_0) was 0.72 for deflection and 0.65 for stress, making it the second most influential parameter. Site practices that permit early application of superimposed loads or post-tensioning at ages as low as 3 to 7 days should be discouraged. Enforcing a minimum age at stressing of 28 days and a minimum age at full loading of 60 days would reduce the predicted creep coefficient by 20 to 35% relative to early-loading scenarios.

Table 5. Summary Comparison: Current Design Practice vs. Recommendations of This Study

Design Parameter	Current Practice (Typical)	Recommended (This Study)	Improvement
Minimum concrete grade (tropical spans > 30m)	f_ck = 25 MPa	f_ck = 35 MPa	-22% creep
Age at stressing (minimum)	No requirement (often 3–7 days)	28 days	-20 to -35% phi
Creep coefficient model	CEB-FIP MC2010 uncorrected	CEB-FIP * k_T * k_RH	+Accuracy in tropics
Serviceability check horizon	50 years	100 years	Full lifecycle
Shrinkage RH design value	RH = 65% (EN 1992-1-1)	RH = 40% (dry season)	+93% epsilon_sh

Source: Author compilation based on EN 1992-2, ACI 318-19, and results of this study.

8. CONCLUSIONS

This paper has presented a comprehensive analytical, numerical, and parametric investigation of time-dependent creep and shrinkage effects on pre-stressed concrete bridge decks, with specific attention to the tropical and sub-Saharan African environmental conditions under which bridge infrastructure in

South Sudan and the East African Community is increasingly being designed and built. The principal conclusions are as follows:

First, the CEB-FIP MC2010 creep model, when applied without climate correction to tropical conditions (T = 30°C, RH = 40 to 60%), underestimates the final creep coefficient by approximately 12 to 28% compared to experimentally calibrated predictions. The proposed tropical correction factors k_T and k_RH (Equations 16 and 17) provide a simple but physically motivated correction that should be adopted for regional practice.

Second, total time-dependent prestress losses over a 100-year service life range from 14.2% (C40/50 concrete) to 20.9% (C28/35 concrete) of the initial jacking force at the baseline tropical condition. These values are systematically higher than the 15% typically assumed in temperate-climate design, and the shortfall increases further under extreme arid conditions.

Third, the sensitivity analysis identifies relative humidity and age at loading as the two most dominant parameters controlling long-term deflection, together accounting for over 75% of the total parametric variance in predicted midspan deflection. These parameters should receive explicit and conservative treatment in design specifications for tropical bridge infrastructure.

Fourth, the finite element time-stepping analysis demonstrates that serviceability limits of L/250 are satisfied over a 100-year life for concrete grades of 32 MPa and above at the baseline tropical condition, but approach critical values (less than 40% margin) for lower-grade concrete under dry-season RH conditions of 40% or less. Design engineers in the region should systematically check deflection at the minimum anticipated humidity rather than the annual mean.

Future work should focus on field instrumentation of in-service pre-stressed bridges in South Sudan and East Africa to validate and further calibrate the proposed correction factors, and on extending the current analysis framework to composite (concrete-steel) bridge decks and multi-span continuous systems where creep redistribution effects are significantly more complex.

REFERENCES

Abdullahi, M., Ozims, U. A., & Al-Mattarneh, H. (2019). Creep of concrete in tropical climate: field measurements and code predictions. Construction and Building Materials, 218, 310–320.

ACI Committee 209. (1992). Prediction of Creep, Shrinkage, and Temperature Effects in Concrete Structures (ACI 209R-92). American Concrete Institute.

Bazant, Z. P. (1972). Prediction of concrete creep effects using age-adjusted effective modulus method. ACI Journal Proceedings, 69(4), 212–217.

Bazant, Z. P., & Baweja, S. (1995). Creep and shrinkage prediction model for analysis and design of concrete structures: Model B3. Materials and Structures, 28, 357–365.

British Standards Institution. (2004). Eurocode 2: Design of Concrete Structures — Part 2: Bridges (EN 1992-2). BSI.

fib (International Federation for Structural Concrete). (2013). fib Model Code for Concrete Structures 2010. Ernst & Sohn, Berlin.

Gilbert, R. I., & Mickleborough, N. C. (1990). Design of Prestressed Concrete. Unwin Hyman, London.

Gilbert, R. I., & Ranzi, G. (2011). Time-Dependent Behaviour of Concrete Structures. Spon Press, London.

Guo, T., Frangopol, D. M., Chen, Y., & Zhang, W. (2020). Monitoring of creep and shrinkage in large-scale post-tensioned concrete girders under field conditions. Engineering Structures, 207, 110251.

Lin, T. Y., & Burns, N. H. (1981). Design of Prestressed Concrete Structures (3rd ed.). Wiley, New York.

Magura, D. D., Sozen, M. A., & Siess, C. P. (1964). A study of stress relaxation in prestressing reinforcement. PCI Journal, 9(2), 13–57.

Nawy, E. G. (2010). Prestressed Concrete: A Fundamental Approach (5th ed.). Prentice Hall, New Jersey.

Neville, A. M. (2011). Properties of Concrete (5th ed.). Pearson Education, Harlow.

Ranisch, E. H. (1982). Redistribution of moments in continuous pre-stressed concrete structures due to creep. Beton- und Stahlbetonbau, 77(11), 283–288.

Wong, S. F., & Wee, T. H. (2000). Shrinkage of high-strength concrete in a tropical environment. Magazine of Concrete Research, 52(4), 293–302.

World Bank. (2022). South Sudan Infrastructure Assessment Report. World Bank Group, Washington, D.C.

Dilger, W. H. (1982). Creep analysis of prestressed concrete structures using creep-transformed section properties. PCI Journal, 27(1), 98–118.

CEN. (2004). Eurocode 2: Design of Concrete Structures — Part 1-1: General Rules (EN 1992-1-1). European Committee for Standardization.

Trost, H. (1967). Implications of the superposition principle for creep and relaxation problems in concrete and reinforced concrete. Beton- und Stahlbetonbau, 62(10), 230–238.

Branson, D. E. (1977). Deformation of Concrete Structures. McGraw-Hill, New York.

Comite Euro-International du Beton. (1978). CEB-FIP Model Code 1978 for Concrete Structures. CEB, Lausanne.

Bažant, Z. P., & Panula, L. (1980). Creep and shrinkage characterization for analyzing prestressed concrete structures. PCI Journal, 25(3), 86–122.

Elices, M., Planas, J., & Guinea, G. V. (1992). Shrinkage eigenstresses in concrete beams: analytical and numerical analysis. Cement and Concrete Research, 22(1), 77–94.

Ozbolt, J., & Reinhardt, H. W. (2001). Sustained loading strength of concrete: modelling and experiments. Journal of Advanced Concrete Technology, 1(2), 143–152.

Tadayon, M. H., Khaloo, A. R., & Amini, E. (2011). Long-term deflection of reinforced concrete beams: combined effects of creep, shrinkage and non-linear cracking. Magazine of Concrete Research, 63(9), 667–678.

Received: [Date] | Revised: [Date] | Accepted: [Date] | Published: [Date]